Photochemistry and Photobiology, Vol. 62, No. 2, pp. 299–308, 1995
Printed in the United States. All rights reserved

0031-8655/95 $05.00+0.00

THE ORIENTATION OF THE TRANSITION DIPOLE MOMENTS OF CHLOROPHYLL *a* AND PHEOPHYTIN *a* IN THEIR MOLECULAR FRAME

M. A. M. J. VAN ZANDVOORT*, D. WRÓBEL†, P. LETTINGA, G. VAN GINKEL and Y. K. LEVINE
Debye Institute, Buys Ballot Laboratory, Princetonplein 5, 3584 CC Utrecht, the Netherlands

(*Received* 24 *October* 1994; *accepted* 22 *March* 1995)

Abstract—In this paper we describe the determination of the orientation of the absorption and emission transition dipoles of chlorophyll *a* and pheophytin *a* in their molecular frame. For this purpose we have embedded the pigments in anhydrous nitrocellulose films with a concentration of 2×10^{-7} mol/g. We have shown previously that under these conditions the pigments are in a purely monomeric state, are distributed uniformly both before and after stretching and that no intermolecular energy transfer among the molecules takes place.

Using a combination of steady-state anisotropy experiments on unstretched films and angle-resolved fluorescence depolarization measurements on stretched films, we obtain the orientation of the transition dipole moments of both pigments in their molecular frame and the orientational distribution function of the molecules relative to the stretching direction of the film.

The steady-state anisotropy measurements indicate that chlorophyll *a* has two distinct emission dipole moments and that excitation in the Soret-region results in simultaneous excitation of two or more absorption transition dipole moments. On the other hand, excitation in the Q_Y-band involves only a single dipole moment. The directions of the transition dipole moments in the molecular frame are obtained from the angle-resolved measurements. Pheophytin *a* also exhibits two emission dipole moments, but the angle between them is much smaller than that between the corresponding dipoles for chlorophyll *a*. As a consequence the dipole moments contributing to the Soret-region could not be resolved and only an effective absorption transition dipole moment in the Soret-region is extracted.

INTRODUCTION

The interest in the spectroscopic characteristics of chlorophyll *a* (Chl *a*)‡ and pheophytin *a* (Pheo *a*) originates in their central role in the photosynthetic process. Chlorophyll *a* is the main pigment in the light-harvesting complexes in green plants and most algae.[1] Furthermore, a special pair of Chl *a* pigments is the primary acceptor in the photosynthetic reaction center[2,3] where charge separation takes place. Pheophytin *a* is the major degradation product of Chl *a* and also functions as an acceptor in the electron transport chain in reaction centers.[2,3]

The spectroscopic properties of assemblies of chlorophyll pigments are widely studied in model systems under controlled experimental conditions.[4,5] In these studies (polarized) fluorescence techniques are often used, not only because they yield information about the aggregation and degradation state of the pigments, but also because the time window of the technique captures intermolecular energy transfer (ET) processes.[4,5] The efficiency of these ET processes is determined by the photophysical properties of the pigments as expressed in the Förster transfer rates[6,7] and the orientation factor κ^2. The latter factor contains the mutual orientations of the transition dipole moments of the donor and the acceptor pigments. Knowledge of κ^2 is prerequisite for the description of ET processes in ordered systems. The evaluation of the orientation factor is not straightforward in many cases, since it involves an averaging over both the orientational order and rotational dynamics of the pigments on the timescale of the fluorescence lifetime.[8–12] Moreover, in orientationally anisotropic systems this can only be carried out if the directions of the transition moments in the molecular frame are known.

For this reason much theoretical and experimental attention has been paid to the determination of the directions of the transition dipole moments in the frame of the highly asymmetric chlorophyll molecules. These studies were primarily concerned with the understanding of the absorption spectrum in terms of electronic states of the pigments. It was shown on the basis of the symmetry properties of dipole-allowed π–π^* transitions that the absorption dipole moments lie along one of the two orthogonal effective symmetry axes of the porphyrin ring.[13–15] Linear dichroism experiments on chlorophylls in partially ordered matrices were indeed used for the assignment of the absorption spectral bands to the orthogonal transition moments.[16–21] Moreover, similar reasoning showed that the emission dipole moments could only lie either parallel or perpendicular to absorption dipole moments. As a consequence, the fluorescence anisotropy of chlorophylls was predicted to be either 0.4 (parallel moments) or −0.2 (perpendicular moments). The observation that the anisotropy varies between these limits across the

*To whom correspondence should be addressed.
†Present address: Institute of Physics, Poznań Technical University, Piotrowo 3, 60-965-Poznań, Poland.
‡*Abbreviations:* AFD, angle-resolved fluorescence depolarization experiment; Chl *a*, chlorophyll *a*; DMSO, dimethylsulfoxide; ET, energy transfer; NC, nitrocellulose; Pheo *a*, pheophytin *a*.

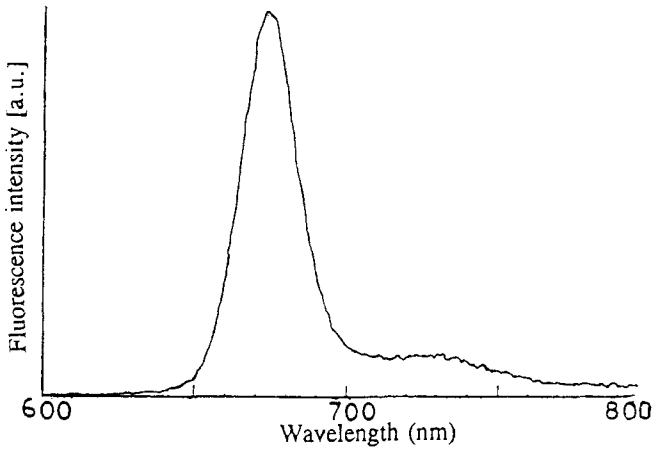

Figure 1. Emission spectra of Chl *a*.

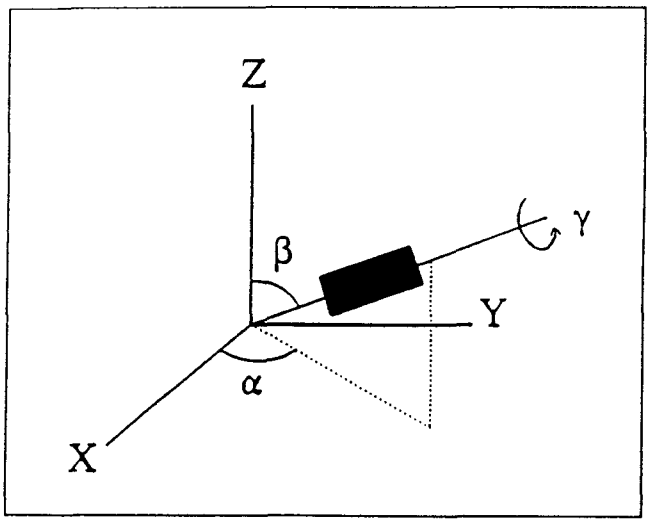

Figure 2. Definition of Euler angles.

absorption spectrum was and is attributed to the overlap of orthogonal transitions.

It was noted, however, that the limiting values of the anisotropy were not experimentally observed for any pigment molecule, including the chlorophylls, and this has been the cause of extended discussions in the literature up to now.[22,23] It is now recognized that even in symmetric planar molecules both the absorption and emission transition dipoles can have an off-axis orientation.[24–26] Additionally, the complex photophysics of chlorophyll molecules is demonstrated by the unexpected variation of the fluorescence anisotropy across the emission band (for reference the emission spectrum of Chl *a* is given in Fig. 1). The emission spectrum of Pheo *a* is very similar). This has been attributed to overlapping (off-axis) fluorescence transitions.[27–30]

Clearly, a number of questions about the photophysics of chlorophyll molecules still need to be answered. In particular the nature of the transition dipole overlap and the orientation of the dipole moments in the molecular frame require further investigation. To this end we have undertaken a study of Chl *a* and Pheo *a* embedded in anhydrous nitrocellulose (NC) matrices in which rotational motions are quenched. We have shown previously[4,5] that the pigments are in the monomeric state in both unstretched and stretched films. These systems are amenable for the determination of molecular properties because at low concentrations, below 3×10^{-7} mol/g, no ET processes take place. We shall here furthermore exploit a combination of steady-state anisotropy experiments on unstretched films and angle-resolved fluorescence depolarization (AFD) experiments on stretched films in order to characterize the directions of the transition dipole moments. Moreover, the mode of orientation of the Chl *a* and Pheo *a* chromophores is addressed. Special attention is paid to the question of mixed transitions and it is demonstrated that the applied combination of techniques, steady-state anisotropy and AFD experiments affords the entanglement of the contributions from different absorption dipole moments to the mixed Soret absorption band.

THEORY

We shall here discuss the theoretical background of steady-state fluorescence depolarization experiments with reference to the determination of the orientation of the transition dipole moments of Chl *a* and Pheo *a* in their molecular frame. The underlying assumptions will be discussed and the theory will be extended to the situation of mixed transitions.

General theory of fluorescence polarization.

The dipole–dipole character of the interaction between light and pigments implies that the absorption and emission of light can be described by the unit vectors $\hat{\mu}$ and $\hat{\nu}$, respectively.[31] The probability of excitation by light of low intensity with polarization direction $\hat{e}_i$ is given by Fermi's golden rule[31] as

$$P_t \propto (\hat{e}_i\hat{\mu})^2. \tag{1}$$

Similarly, the probability of emission of light with polarization direction $\hat{e}_f$ is described by:

$$P_e \propto (\hat{e}_f\hat{\nu})^2. \tag{2}$$

For a system in which the pigments neither reorient nor exhibit ET on the timescale of the fluorescence lifetime, the intensity of fluorescence under steady-state illumination is now given by[32]

$$I_{if} = k \int \frac{d\Omega}{8\pi^2} (\hat{e}_f\hat{\nu})^2(\hat{e}_i\hat{\mu})^2 f(\Omega). \tag{3}$$

Here k is determined by the excitation light intensity and pigment concentration while $f(\Omega)$ is the orientational distribution function of the pigment molecules within the sample. Here Ω denotes the three Euler angles (α, β, γ), defining the orientation of the pigment (see Fig. 2). The integral is thus just an average of the absorption and emission probabilities over all the molecular orientations in the ensemble.

The disentanglement of geometrical factors and molecular properties

The intensities observed in fluorescence depolarization experiments, Eq. 3, are expressed in terms of the polarization of the (incident and emitted) light in the laboratory frame and the orientations of the (absorption and emission) dipole

moments in the sample frame. However, this latter orientation is in fact determined by the orientation of the molecules in the sample since the transition dipoles are rigidly attached to the molecule. In order to link the experimental geometry, the molecular orientation in the sample and the orientation of the transition dipole moments in the molecular frame, we carry out two rotational transformations: (laboratory frame → sample frame) and (molecular frame → sample frame). The rotations are most conveniently expressed in terms of the orthogonal set of Wigner rotation matrix elements $D^L_{mn}(\Omega)$,[33] especially because the scalar products in Eq. 3 can be expressed in terms of the Wigner rotation element D^2_{00}

$$(\hat{e}_i\hat{\mu})^2 = \frac{2D^2_{00}(\hat{e}_i\hat{\mu}) + 1}{3} \tag{4}$$

$$(\hat{e}_f\hat{\nu})^2 = \frac{2D^2_{00}(\hat{e}_f\hat{\nu}) + 1}{3} \tag{5}$$

after some laborious but straightforward algebra and making use of the notation

$$\langle(\ldots)\rangle = \int \frac{d\Omega}{8\pi^2}(\ldots)f(\Omega)$$

we obtain

$$I_{if} = k\Big[1 + 2D^{2*}_{00}(\Omega e_i)S_\mu + 2D^2_{00}(\Omega e_f)S_\nu + 4\sum_{k=-2}^{2} D^{2*}_{k0}(\Omega e_i)D^2_{k0}(\Omega e_f)G_k\Big] \tag{7}$$

with Ω_{e_i} the Euler angle of the polarization direction of exciting light in the laboratory frame and Ω_{e_f} the Euler angle of the polarization direction of emitted light in the laboratory frame.

$$S_\mu = \sum_{i=-2}^{2} \langle D^2_{0i}(\Omega_{sm})\rangle\, D^2_{i0}(\Omega_\mu) \tag{7a}$$

$$S_\nu = \sum_{j=-2}^{2} \langle D^{2*}_{0j}(\Omega_{sm})\rangle\, D^{2*}_{j0}(\Omega_\nu) \tag{7b}$$

$$G_k = \sum_{i,j=-2}^{2} \langle D^{2*}_{kj}(\Omega_{sm})D^2_{ki}(\Omega_{sm})\rangle\, D^{2*}_{j0}(\Omega_\nu)D^2_{i0}(\Omega_\mu) \qquad k = 0,1,2 \tag{7c}$$

where Ω_{sm} is the orientation angle of the fluorescent molecule in the sample frame; $\Omega\mu$ ($\Omega\nu$) is the orientation of the absorption (emission) moment in the molecular frame. Equations 7 express the separation of the geometrical factors Ω_{e_i} and Ω_{e_f} (dictated by the experimental setup) from the molecular properties (the order parameters S_μ and S_ν and the correlation functions G_k). The experimental setup will be considered in the next section and we shall here confine ourselves to the molecular properties.

The order parameters S_μ and S_ν are determined by the orientation of the corresponding dipole moment in the molecular frame as well as the orientational distribution of the molecule in the sample. The latter is given in terms of the molecular order parameters $\langle D^l_{mn}(\Omega_{sm})\rangle$. In our situation of quenched reorientational motions, the correlation functions G_k can be expressed in the order parameters of rank two and four (1 = 2 and 1 = 4, respectively), using the Clebsch Gordan series.[29,33–35] If we furthermore assume the orientational distribution of the pigments in the polymer matrix to be either isotropic or uniaxially symmetric about the stretching direction we find that $G_k = G_{-k}$.[36]

Equation 7 now indicates that a fluorescence depolarization experiment yields a maximum of five independent parameters, namely S_μ, S_ν, G_0, G_1 and G_2. These parameters contain all the accessible molecular information (order parameters and transition dipole moment directions).

The question now arising is how to extract this information from the five experimental parameters. For the planar porphyrin ring the in-plane absorption and emission dipole are defined by the two Euler angles β_μ and β_ν. The choice of the molecular z-axis in the ring allows us to set α_μ and α_ν to zero. The main difficulty now is that in principal up to 25 second rank and 81 fourth rank order parameters need to be determined. However, many of these are identically zero for reasons of symmetry.[29,32,34,37] For films stretched uniaxially along the Z-axis, the distribution of the planar pigments is invariant under rotations around this axis, possesses mirror symmetries in the XY- and XZ-plane of the film and, moreover, is invariant to reflections in the xz- and yz-molecular frames. Consequently, only five non-zero order parameters remain

$$\langle P_2\rangle = \langle D^2_{00}\rangle, \quad \langle P_4\rangle = \langle D^4_{00}\rangle, \quad \langle D^2_{02}\rangle, \quad \langle D^4_{02}\rangle, \quad \langle D^4_{04}\rangle.$$

Of these five order parameters the first three are assumed to be the most significant in the description of the orientational distribution function $f(\Omega)$. The smoothest possible distribution function that is consistent with these three order parameters may be reconstructed with the maximum entropy formalism[29,35,38] given by

$$f(\Omega) = A\exp[\lambda_2 P_2(\beta_{sm}) + \lambda_4 P_4(\beta_{sm}) + \epsilon\sin^2(\beta_{sm})\cos(2\gamma_{sm})] \tag{8}$$

with A a normalization constant; λ_2, λ_4 and ϵ are the adjustable variables whose values are uniquely related to the three order parameters.

The approach outlined above now expresses the five experimental parameters S_μ, S_ν, G_0, G_1, G_2 in terms of three variables (λ_2, λ_4, ϵ) describing the orientational distribution of the pigments relative to the stretching direction and two variables (β_μ and β_ν) defining the orientation of the transition dipole moments relative to the in-plane z-axis of the porphyrin ring.

Steady-state anisotropy experiments on unstretched films

In unstretched films S_μ and S_ν are identically zero, since the pigments have no preferential orientation in the film. An additional consequence of the random orientation is that the three correlation functions are equal and are only determined by the difference angle $\beta_{\mu,\nu}$ between the absorption and emission transition dipole moment in the molecular frame[29,30]

$$G_0 = G_1 = G_2 = 0.2P_2(\cos\beta_{\mu,\nu}). \tag{9}$$

The steady-state fluorescence anisotropy $\bar{r}$ is given by

$$\bar{r} = \left(\frac{I_{VV}}{I_{VH}} - 1\right)\Big/\left(\frac{I_{VV}}{I_{VH}} + 2\right) \tag{10}$$

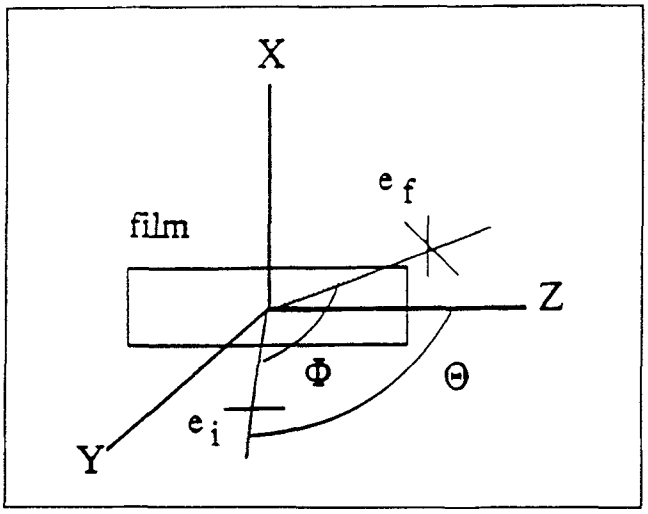

Figure 3. Experimental set-up for AFD experiments on stretched films.

where the subscripts denote the polarization directions of the exciting and emitted light, respectively, in the laboratory frame. Using Eq. 9 and filling in the proper geometrical factors in Eq. 7 and 10 gives

$$\bar{r} = 0.4P_2(\cos \beta_{\mu,\nu}) \tag{11}$$

independent of the chosen scattering geometry using vertically polarized incident light. Thus anisotropy experiments on unstretched films only yield the difference angle between the absorption and emission dipole moments in the molecular frame.

AFD experiments on stretched films

The setup for this experiment is shown schematically in Fig. 3. Note that the stretching direction of the film is horizontal. The ratio $R_e = I_{HH}/I_{HV}$ is measured as a function of θ and ϕ, where θ denotes the angle between the direction of the exciting beam and the stretch direction of the film and θ denotes the angle between the direction of the polarized fluorescence emission and the excitation light beam. Under these conditions Eq. 7 yields[29,32]

$$\frac{1}{R_e} = \frac{\begin{array}{l}1 + 2S_\mu + 2S_\nu + 4G_0 \\ - 3(S_\mu + 2G_0)\sin^2\theta - 3(S_\nu + 2G_0)\sin^2\phi \\ + 3G_1 \sin 2\theta \sin 2\phi + 3(G_2 + 3G_0)\sin^2\phi \sin^2\theta\end{array}}{1 + 2S_\mu - S_\nu - 2G_0 - 3(S_\nu - G_0 + G_2)\sin^2\phi}. \tag{12}$$

Because all five parameters S_μ, S_ν, G_0, G_1, G_2 appear in the expression for $1/R_e$, they can be determined in an AFD experiment. Making use of a suitable analysis method, from these five parameters the orientational distribution function and the orientation of the dipole moments in the molecular frame can be determined.

Theory of mixed transitions

In the preceding treatment we have explicitly assumed each absorption and each emission band of the pigment to be pure. Thus, the excitation transition within a given band is described with a single absorption dipole moment. Similarly only one dipole moment is needed to describe the emission transition of a given band. While this may suffice for symmetric molecules, it is not necessarily the case for chlorophyll molecules.[39,40] We shall here disregard the underlying photophysical processes involved and simply adopt an operational approach in which the transitions are characterized by a linear superposition of dipole moments with different orientations in the molecular frame.[29]

For illumination at one wavelength now n dipole moments are excited with dipole p having a weight f_p. Similarly, emission at a single wavelength arises from m dipoles with dipole q having weight g_q. In analogy with Eq. 3, the intensity under steady-state conditions is now given by

$$I_{if} = k \sum_{p,q=1}^{m,n} f_p g_q \langle (\hat{e}_i \hat{\mu})^2 (\hat{e}_f \hat{\nu})^2 \rangle. \tag{13}$$

The structure of Eq. 7 is conserved, but now S_μ, S_ν, G_k are given by

$$S_\mu = \sum_{i=-2}^{2} \langle D_{0i}^2(\Omega_{sm}) \rangle \sum_{p=1}^{n} f_p D_{i0}^2(\Omega_{\mu,p}) \tag{13a}$$

$$S_\nu = \sum_{j=-2}^{2} \langle D_{0j}^{2*}(\Omega_{sm}) \rangle \sum_{q=1}^{m} g_q D_{j0}^2(\Omega_{\nu,q}) \tag{13b}$$

$$G_k = \sum_{i,j=-2}^{2} \langle D_{kj}^{2*}(\Omega_{sm}) D_{ki}^2(\Omega_{sm}) \rangle \times \sum_{p,q=1}^{m,n} f_p g_q D_{i0}^2(\Omega_{\mu,p}) D_{j0}^{2*}(\Omega_{\nu,q}) \tag{13c}$$

where $\Omega_{\mu,p}$, $\Omega_{\nu,q}$ are the orientations of, respectively, absorption dipole moment p and emission dipole q in the molecular frame.

It is clear that although Eq. 13a–13c are analogous to Eq. 7a–7c, many new variables (f_p, g_q, with p, q ranging from 1 to n and m, respectively) enter the expressions for the experimentally accessible parameters at a given combination of excitation and emission wavelengths. In order to limit the number of unknown variables, we shall use the model advanced by van Gurp and coworkers[29,30] to account for the fluorescence anisotropy of Chl *a* in castor oil and lipid bilayers. This model will be justified *a posteriori*. The model takes the emission spectrum to arise from two pure transitions, one centered at 680 nm, $\hat{\nu}_1$, and one centered at 730 nm, $\hat{\nu}_2$. In addition the Q_Y absorption band of Chl *a* and Pheo *a* are taken to be pure and characterized by an absorption dipole moment $\hat{\mu}_{652}$. Finally, the Soret-regions of Chl *a* and Pheo *a* are assumed to arise from two overlapping absorption dipole moments $\hat{\mu}_{s1}$, $\hat{\mu}_{s2}$ with weight f_1, $(1 - f_1)$, respectively. The value of f_1 varies over the Soret-region and is thus dependent on the excitation wavelength. In contrast to the model proposed in van Gurp and coworkers,[29,30] the two dipole moments need not be perpendicular.

Although the number of variables entering the parameters S_μ, S_ν, G_0, G_1, G_2 is significantly reduced, seven variables still determine the value of the five experimental parameters for a given combination of excitation and emission wavelength in an impure band. This problem can be circumvented using a global data analysis approach in which measure-

ments obtained using different combinations of excitation and emission wavelengths are linked.[32]

MATERIALS AND METHODS

Sample preparation. Chlorophyll *a* was extracted from spinach leaves (either obtained from the local market or cultivated in the laboratory) according to the method described by Terpstra and Lambers[41] and purified using thin-layer chromatography. Pheophytin *a* was obtained from Chl *a* using a standard procedure.[42]

Acetone and dimethylsulfoxide (DMSO) of analytical grade purity were purchased from E. Merck and from J. T. Baker Chemicals B.V., respectively, and used without further purification. Nitrocellulose powder was obtained from Wolff Walsroder A.G. and purified before use in the following way: NaOH with a final concentration of 0.01 *M* was added to NC powder and kept in the dark under continuous stirring for 20 h. The mixture was then cleaned several times with water and dried at room temperature under a continuous nitrogen stream. Using this method acid traces and radicals in the NC powder were removed. Pigment–polymer–DMSO solutions are prepared by mixing 5 mL DMSO with the desired amount of dried pigment. Then the NC powder is added, followed by stirring for 15 min at room temperature. The amount of NC is 0.3 g per 5 mL DMSO. From these solutions films were obtained by the same evaporation procedure as used for PVA films.[4] The NC films were stretched using a home-built apparatus. The films were allowed to equilibrate with saturated DMSO vapor for 2 h before stretching at room temperature. Traces of DMSO were removed by drying the stretched films under nitrogen atmosphere. Uniaxiality was tested with the methods described there. Final concentration of both Chl *a* and Pheo *a* in the film was 2×10^{-7} mol/g.

Experiments. Steady-state anisotropy and AFD experiments were carried out on a home-built setup as described by van Gurp *et al.*,[35] but using photon counting detection. Anisotropy measurements on unstretched films were carried out using the pre-set angle combination $\theta = 40°$, $\phi = 10°$. The AFD experiments on stretched films for a given combination of excitation and emission wavelength yielded $1/R_e$ utilizing 60 combinations of θ and ϕ. Scattered light was totally suppressed using a combination of an excitation monochromator with bandwidth of 3 nm and excitation and emission filters (Omega Optics, bandwidth 3 nm). Anisotropy excitation spectra for both Chl *a* and Pheo *a* were measured for two emission wavelengths: 680 nm and 730 nm. The AFD measurements on Chl *a* utilized the following combinations of excitation and emission wavelengths: (380, 680) nm, (380, 730) nm, (445, 680) nm, (445, 730) nm, (652, 680) nm and (652, 730) nm, while for Pheo *a* the combinations were (370, 680) nm, (414, 680) nm, (652, 680) nm.

The AFD results of the six wavelength combinations for Chl *a* or the three wavelength combinations for Pheo *a* were simultaneously fitted using a Global target approach,[43] using the nonlinear least-squares Marquardt procedure (ZXSSQ) from the IMSL library. The measured ratios were fitted directly to the distribution function variables and the directions of the transition dipole moments.

RESULTS

The theoretical expressions for the steady-state fluorescence anisotropy and the AFD ratios indicate that a maximum of five experimental parameters can be obtained from the measurements. Yet these parameters are determined by up to seven variables describing the molecular orientational order and directions of the transition dipole moments. In order to extract these parameters, it is now necessary to design the experimental protocol using suitable combinations of absorption and emission wavelengths in such a way that each combination provides more independent experimental parameters than introducing new adjustable variables.

Because all the measurements are carried out on a single sample the three adjustable variables describing the molecular orientational distribution are independent of the combination of excitation and emission wavelength. Furthermore, excitation at one wavelength and observation at two distinct emission wavelengths yields four independent parameters, at the cost of only one new adjustable variable. Similarly, the observation at one emission wavelength and excitation at two distinct wavelengths in the Soret-region yields four new independent parameters, but again only one new variable enters their description. In order to extract the maximum amount of independent information we have measured $1/R_e(\theta, \phi)$ at the following combinations of excitation and emission wavelengths:

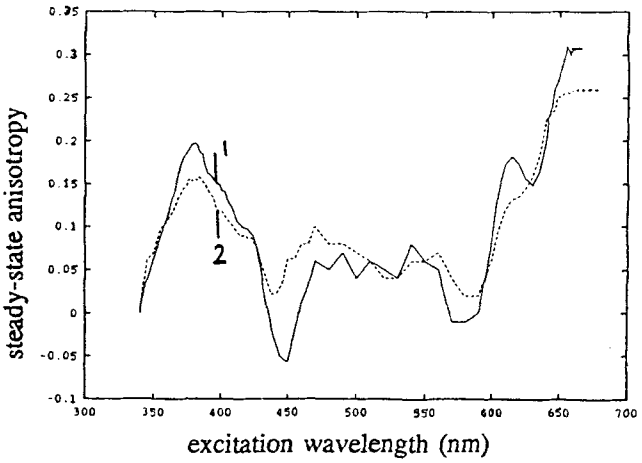

Figure 4. Excitation anisotropy for Chl *a*/NC, 2×10^{-7} mol/g: 1—emission wavelength 680 nm; 2—emission wavelength 730 nm.

—Excitation in the Soret-region, emission at 680 nm:
$S_\mu(\lambda_{exc})$, S_{ν_1}, $G_{0,\nu_1}(\lambda_{exc})$, $G_{1,\nu_1}(\lambda_{exc})$, $G_{2,\nu_1}(\lambda_{exc})$ are fully determined by
λ_2, λ_4, ϵ, β_{ν_1}, $f_1(\lambda_{exc})$, $\beta_{\mu s_1}$, $\beta_{\nu s_2}$

—Excitation in the Soret-region, emission at 730 nm:
$S_\mu(\lambda_{exc})$, S_{ν_2}, $G_{0,\nu_2}(\lambda_{exc})$, $G_{1,\nu_2}(\lambda_{exc})$, $G_{2\nu_2}(\lambda_{exc})$ are fully determined by
λ_2, λ_4, ϵ, β_{ν_2}, $f_1(\lambda_{exc})$, $\beta_{\mu s_1}$, $\beta_{\nu s_2}$

—Excitation in the Q_Y-band, emission at 680 nm:
$S_{\mu_{652}}$, S_{ν_1}, $G_{0,\nu_1}(\mu_{652})$, $G_{1,\nu_1}(\mu_{652})$, $G_{2,\nu_1}(\mu_{652})$ are fully determined by
λ_2, λ_4, ϵ, β_{ν_1}, $\beta_{\mu_{652}}$

—Excitation in the Q_Y-band, emission at 730 nm:
$S_{\mu_{652}}$, S_{ν_2}, $G_{0,\nu_2}(\mu_{652})$, $G_{1,\nu_2}(\mu_{652})$, $G_{2,\nu_2}(\mu_{652})$ are fully determined by
λ_2, λ_4, ϵ, β_{ν_2}, $\beta_{\mu_{652}}$

In order to determine the most suitable excitation wavelengths in the Soret-band, we have carried out fluorescence anisotropy measurements on unstretched films.

The excitation spectra of the steady-state anisotropy of Chl *a* for observation at 680 nm and 730 nm are shown in Fig. 4. The corresponding spectra for Pheo *a* are shown in Fig. 5. The spectra for the two emission wavelengths differ significantly for Chl *a*. This observation underpins our model for Chl *a* where two distinct dipole moments contribute to the emission spectrum. From the difference in anisotropy at the two emission wavelengths the difference angle between the two corresponding emission moments can be estimated to be 5°. At wavelengths in the Soret-band below 410 nm

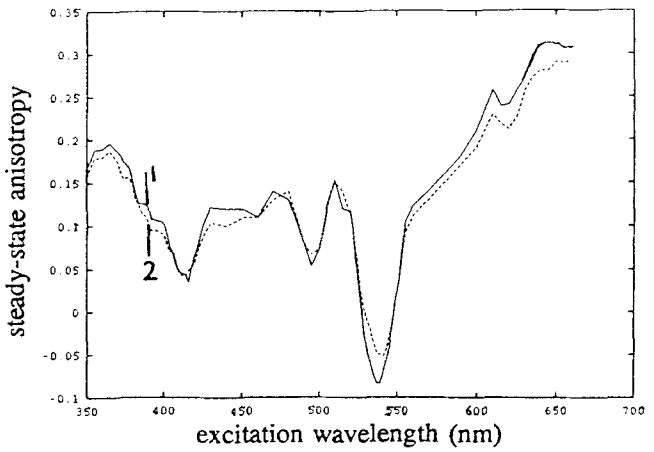

Figure 5. Excitation anisotropy for Pheo *a*/NC, 2×10^{-7} mol/g: 1—emission wavelength 680 nm; 2—emission wavelength 730 nm.

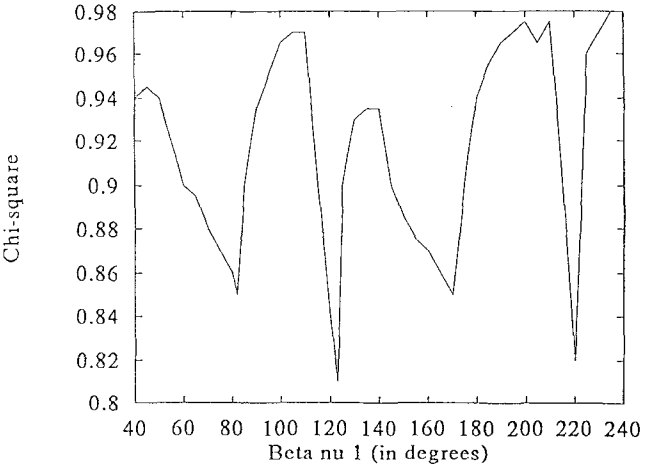

Figure 6. The χ^2 profile AFD measurement Chl *a*/NC, 2×10^{-7} mol/g.

the anisotropy observed at 680 nm is higher than that found at 730 nm, while for wavelengths above 410 nm the reverse is true. The value of the anisotropy at the cross-over point at 410 nm, 0.08, indicates that the two transition dipole moments in the Soret-band are almost perpendicular.[30] The sensitivity of the AFD experiment to the orientations of the absorption transition dipole moments can now be increased by choosing two wavelengths on either side of the cross-over point. To this end we excited the Chl *a* molecules in the stretched film at 380 nm and 440 nm.

In contrast, for Pheo *a*, the differences are much smaller and a difference angle between the two emission moments of only 2° can be calculated. Because this is smaller than the experimental errors, this difference is not significant. The absence of a significant dependence of the excitation spectrum of the fluorescence anisotropy for Pheo *a* indicates that effectively only a single dipole moment contributes to the emission band. Consequently, it is not possible to resolve the contribution from different absorption dipole moments in the Soret-region and only the orientation of an effective dipole moment can be obtained from the experiments.

The fluorescence anisotropy spectra (Figs. 4 and 5) indicate furthermore that the Q_Y-band of both Chl *a* and Pheo *a* are pure. This can be seen from the observation that the anisotropy reaches a plateau at 650 nm with a constant difference in its value between observation at 680 nm and 730 nm. Again, the small difference in the plateaus of the anisotropy for Pheo *a* implies a single effective emission dipole moment. The values of the anisotropy across the absorption spectrum found here correspond to those reported earlier by us from time-resolved experiments.[5]

The AFD experiments on Chl *a* samples yielded six datasets each containing 60 depolarization ratios. With our choice of excitation and emission wavelengths 10 adjustable variables now need to be recovered from a simultaneous fit. The χ^2 surface as a function of the angle between the emission dipole at 680 nm and the molecular z-axis, β_{v_1}, is shown in Fig. 6. The four solutions describe the same physical situation, but each minimum corresponds to a different choice of the z-axis in the porphyrin ring. Consequently, each solution yields a different orientational distribution function and dipole orientation relative to this axis (Table 1). Importantly, the distribution functions extracted are related to one another through a simple rotational transformation involving the difference angle between the corresponding molecular z-axes. This demonstrates unequivocally that the solutions found are self-consistent.

The error margins in the values of the variables were estimated from the profile of the χ^2 surface near the minimum. These errors had only a marginal effect on the features of the orientational distribution functions (Fig. 7).

Similarly, seven adjustable variables were recovered from three datasets of 60 depolarization ratios for one Pheo *a* sample. Again four distinct minima were found (Fig. 8), and the values of the recovered variables are listed in Table 2. In marked contrast with the results for Chl *a*, two distinct pairs of orientational distribution functions are recovered, solutions {b d} and {a c} in Fig. 9 and Table 2. Now only the paired solutions are related by a rotational transformation.

DISCUSSION

We have shown here that the theory of steady-state anisotropy and AFD experiments set out above provides a consistent description of the experimental observations on Chl *a* and Pheo *a* embedded in NC polymer films. The theoretical considerations rely on a number of tacit assumptions whose validity has been tested by us previously.[4,5]

There we have shown that the intermolecular interactions are negligible in NC films at pigment concentrations below 3×10^{-7} mol/g. Thus the measured depolarization of fluorescence is not distorted by ET processes. The fluorescence depolarization is wholly attributable to the static, uniform distribution of monomeric pigments in the films since all motion is quenched on the timescale of the fluorescence lifetime. The fact that the monoexponential fluorescence intensity decay of the pigments does not depend on the extent of stretching of the films is consistent with the basic assumption that decay is an intrinsic molecular property.

The orientational distribution functions for Chl *a* in a stretched NC film corresponding to the four solutions in Table 1 are shown in Fig. 7a–d. Each of these functions describes the same physical situation, but with reference to a

Table 1. The orientational distribution functions and the corresponding orientations of the transition dipole moments of Chl *a*

Variable	Solution a	Solution b	Solution c	Solution d
λ_2	0.34 ± 0.11	−0.4 ± 0.2	0.26 ± 0.02	0.03 ± 0.12
λ_4	−1.3 ± 0.2	1.7 ± 0.5	−0.8 ± 0.3	1.2 ± 0.3
ϵ	0.32 ± 0.02	0.20 ± 0.02	−0.01 ± 0.11	0.08 ± 0.02
$\beta_{\nu 1}$ (°)	82 ± 2	123 ± 2	170 ± 2	221 ± 2
$\beta_{\nu 2}$ (°)	87 ± 2	128 ± 2	175 ± 2	225 ± 2
$\beta_{\mu 652}$ (°)	63 ± 2	105 ± 2	149 ± 2	201 ± 2
$\beta_{\mu s1}$ (°)	55 ± 2	96 ± 2	139 ± 2	193 ± 2
$\beta_{\mu s2}$ (°)	133 ± 2	176 ± 2	225 ± 2	272 ± 2
f_1(exc = 380)	0.70 ± 0.03	0.58 ± 0.03	0.70 ± 0.03	0.62 ± 0.03
f_1(exc = 440)	0.00 ± 0.02	0.00 ± 0.02	0.00 ± 0.02	0.00 ± 0.02
χ^2	0.86	0.82	0.85	0.89

different z-axis in the porphyrin ring structure of Chl *a*. The orientations of the transition dipole moments of each solution (Table 1) are also given with respect to that axis. However, the fit procedure does not provide a relation between the z-axis and the geometrical structure of the porphyrin ring. This can only be done by linking the orientational distribution functions to the inertial axis of the Chl *a* molecule.

It has frequently been shown[31,44,45] that planar molecules with a definite in-plane inertial axis in stretched films tend to align themselves with the inertial axis along the uniaxial stretching direction. However, in films stretched to less than four times their original lengths, a small population is found with the inertial axis making an angle of 90° with the stretching direction. Thus the orientational distribution function with the molecular z-axis chosen along the inertial axis will be centered around $\beta = 0°$ with wings at $\beta = 90°$, $\gamma = 0°$. A choice of the in-plane molecular z-axis perpendicular to the inertial axis corresponds to a rotation of the orientational distribution function by 90° in the molecular plane. This yields an orientational distribution function again centered around $\beta = 0°$ but with significantly higher wings at $\beta = 90°$, $\gamma = 0°$. The orientation for $\gamma = 0°$ when $\beta = 90°$ corresponds to the molecular plane lying parallel to the film surface. Furthermore, the γ-independence of the orientational distribution function for $\beta = 0°$ is inherent in the maximum entropy form of the orientational distribution function (Eq. 8) and reflects the uniaxial symmetry of the stretched film around the stretching direction.

The two orientational distribution functions, solutions b and d (Fig. 7), clearly follow this general pattern. We shall therefore identify the orientational distribution function belonging to solution b with the choice of molecular z-axis along the inertial axis and that of solution d with the choice of the molecular z-axis perpendicular to the inertial axis. Because it was previously shown from a combination of experiments and calculations[46] that the inertial axis of Chl *a* is given by axis I in Fig. 7e, this now means that axis I lies preferentially along the stretching axis of the film and is the molecular z-axis corresponding to solution b. Solutions a, c and d now can be attributed to a choice of axis III, IV and II, respectively, as the molecular z-axis. Axis I and axis II are in literature mostly referred to as the molecular X- and Y-axis, respectively.

The orientations of the transition dipole moments in solution b (Table 1) are given relative to axis I. As a conse-

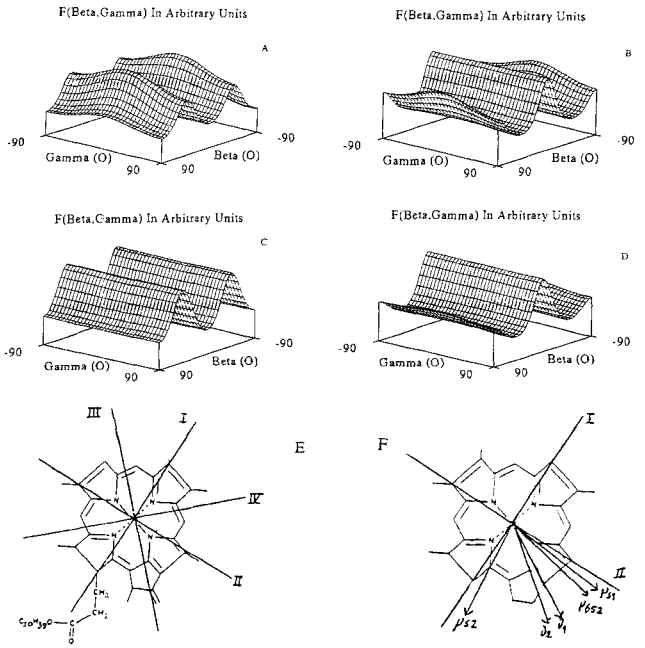

Figure 7. a–d: Orientational distribution functions of Chl *a*/NC, 2 × 10^{-7} mol/g, solutions correspond to Table 1; e, f: Axis definition and orientation of transition dipole moments.

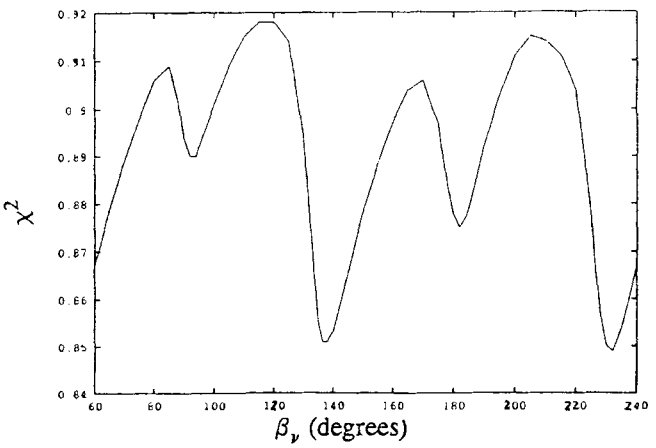

Figure 8. The χ^2 profile of AFD on Pheo *a*/NC, 2 × 10^{-7} mol/g.

Table 2. The orientational distribution functions and the corresponding orientations of the transition dipole moments of Pheo *a*

Variable	Solution a	Solution b	Solution c	Solution d
λ_2	0.77 ± 0.05	1.03 ± 0.01	0.82 ± 0.02	0.49 ± 0.09
λ_4	−0.20 ± 0.05	0.17 ± 0.04	−0.17 ± 0.3	0.18 ± 0.05
ϵ	1.20 ± 0.05	1.07 ± 0.11	−0.99 ± 0.11	1.28 ± 0.11
β_{s1} (°)	92 ± 4	138 ± 3	182 ± 4	232 ± 4
$\beta_{\mu 652}$ (°)	77 ± 6	121 ± 2	167 ± 5	213 ± 2
$\beta_{\mu 414}$ (°)	137 ± 5	182 ± 4	227 ± 4	275 ± 2
$\beta_{\mu 370}$ (°)	63 ± 5	108 ± 3	152 ± 4	199 ± 3
χ^2	0.89	0.85	0.87	0.85

quence of the fact that the four solutions can be interchanged by simple rotational transformations in the plane of the ring, the same absolute orientations of the transition dipole moments in the porphyrin ring are obtained for all four solutions.

The orientations of the transition dipole moments in the porphyrin ring are shown schematically in Fig. 7f. The absorption dipole moment at 652 nm (Q_Y-band) lies close to axis II. The absorption dipole moment μ_{s1} in the Soret-region is also located to axis II, while dipole moment μ_{s2} lies near axis I. Interestingly, at 440 nm only the latter dipole moment is excited. Finally, the orientation of the absorption and emission transition dipole moments and the effective difference angles are in excellent agreement with the results of the steady-state anisotropy measurements. This is a strong indication for the correctness of the model used, because the experimental anisotropy values were not used in the fit procedure of the AFD results.

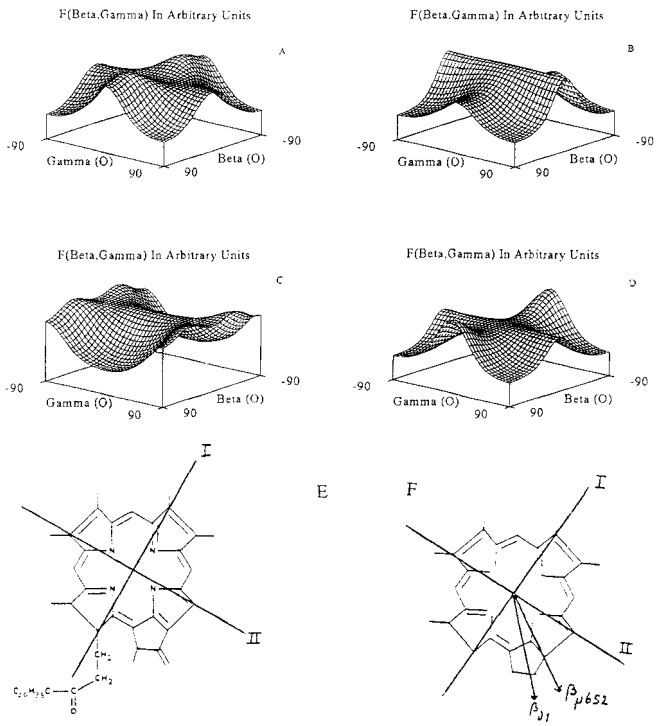

Figure 9. a–d: Orientational distribution functions of Pheo *a*/NC, 2 × 10^{-7} mol/g, solutions correspond to Table 2; e, f: Axis definitions and orientation of transition dipole moments.

The identification of the orientational distribution functions for Pheo *a* (Fig. 9a–d) with the direction of the molecular z-axis in the porphyrin ring follows along similar lines to those described above for Chl *a*. Interestingly, the porphyrin ring of Pheo *a* in the NC film exhibits a markedly smaller degree of orientational order than those for Chl *a*. The reasoning in the case of Pheo *a* is complicated by the finding that the pair of solutions {a c} cannot be converted into the pair {b d} by a simple rotation in the plane of the ring. Thus the two pairs relate to two physically distinct situations. We ascribe this unsatisfactory situation to inherent ambiguities in the numerical analysis. The ambiguities arise from the fact that we are now dealing with a single effective emission transition dipole moment, so that for example the steady-state fluorescence anisotropy is consistent with two distinct directions of this dipole moment in the porphyrin ring. This unfortunately restricts the information about the absorption transition moments that can be extracted from the experimental parameters.

We have identified the solution pair {b d} as the situation corresponding to that found for Chl *a*, with axis I lying preferentially along the stretch direction of the film. With this choice, the molecular z-axes are axis I for solution b and axis II for solution d, the direction of the average absorption dipole moment contributing to the Soret-band of Pheo *a* is obtained. It lies close to the direction of the corresponding dipole moment calculated for the Soret-region of Chl *a*. The absorption dipole moment corresponding to the Q_Y-band is, however, located a little bit further from axis II than for Chl *a*.

The orientations of the transition dipole moments of Chl *a* and Pheo *a* in the porphyrin ring have been obtained here from an operational approach whose basic assumptions are that the absorption and emission transitions of the pigments can be described by a linear superposition of dipole moments. This approach differs from that of earlier studies which relied heavily on the assignment of the absorption spectra to specific photophysical processes. Many authors[16-21] have assumed the (polarized) absorption spectra to consist of transitions polarized either parallel or perpendicular to the X-axis of the porphyrin ring: from the measured linear dichroism and isotropic absorption spectrum the X- and Y-polarized absorption spectra were calculated. These were then fitted to a linear combination of vibronic progressions of main electronic transitions.[16,17] In this way it was found that the Q_Y-band of Chl *a* consists of three Y-polarized progressions, strongly overlapping with a single X-po-

larized progression. Therefore an effective angle of the Q_Y-transition with the molecular Y-axis was calculated. This angle was found to be 20°.[17] In a similar way an effective angle of (16 ± 9)° for Pheo *a* was determined.[17] Both angles are in good agreement with our results. In this respect we also refer to the conclusion of these authors, where it is pointed out that for the determination of the effective angle of the Q_Y-band with the molecular Y-axis, it is not relevant whether only the first progression of the Q_Y-band (Q_Y(0-0)) or the first three progressions of Q_Y are taken to be the equivalent of the Q_X(0-0) band. This further underpins our remark on the pureness of the Q_Y-band above 650 nm. Furthermore, we would like to note that in Norden *et al.*[17] also a weak, X-polarized, band around 630 nm was found. From the pureness of the Q_Y-band above 650 nm, as deduced from our anisotropy measurements, it can be concluded that this band does not attribute intensity above this wavelength. Finally, our results for the Q_Y-band correspond to those reported previously.[18–21] We stress, however, that in all the above-mentioned studies the chlorophyll molecules were assumed to be cylindrically symmetric. We have shown this actually not to be the case, as can be expected for a disk-like molecule. The small discrepancy between the direction for the dipole moments reported here and that reported by our laboratory previously[47] has been tracked down to distortions of the earlier results by scattered light.

From the comparison presented above it becomes clear that is not necessary to *a priori* assume the spectrum of Chl *a* to consist of (partially overlapping) X- and Y-polarized bands. This seems to be particularly important in the analysis of the much more complex Soret-band. In this paper we have analyzed the Soret-band in terms of two overlapping transition dipole moments. Our results do not rule out, however, the possibility that more than two dipole moments contribute. Firstly, the value of the anisotropy at the cross-over point suggests that the two absorption dipole moments in that region make an angle larger than 90°, while an angle smaller than 90° was found here. Secondly, theoretical calculations[13–15] predict a transition dipole to be present at 340 nm. Indeed, a cross-over point is observed at 350 nm.

We have shown here that a combination of steady-state anisotropy measurements and AFD experiments on Chl *a* and Pheo *a* molecules embedded in a monomeric state in stretched NC matrices provide detailed information about the orientational and photophysical properties of the pigments. In particular, this combination affords the separation of the contributions of different dipole moments to the Soret-band. Nevertheless, we have found that this separation can only be achieved if two distinct dipole moments contribute to the emission band. While this is clearly the case for Chl *a*, our results for Pheo *a* have revealed that the difference angle between the emission dipoles is so small that only one effective moment can be extracted from the experiments. For this reason we have only been able to fully characterize Chl *a* but not Pheo *a*. A possible reason for the much smaller difference angle between the two emission moments for Pheo *a* than for Chl *a* might be the influence of the central Mg in the porphyrin ring of the latter.

In this and previous work[5] we have characterized a model system (Chl *a*–NC) suitable for the study of ET processes among the Chl *a* pigments. This system is especially useful for the modeling of the influence of both macroscopical and microscopical orientations on the efficiency of ET. The results reported on in this paper indicate that by uniaxially stretching the NC film, the Chl *a* molecules orient along the stretching direction. Recent advances in the maximal possible stretching amount (five times the original length) have convinced us of the great potentials of the Chl *a*–NC system. Making use of the macroscopical alignment in dilute systems we determined the orientations of the transition dipole moments in the molecular frame and we have argued the relevance of these in the description of ET processes. Already, the first time-resolved experiments on stretched NC films have been carried out, both in the absence and presence of ET. These experiments are now being analyzed.

Acknowledgements—M.A.M.J.Z. was supported by the Dutch Foundation of Chemistry (SON) under the auspices of the Netherlands Organisation of Scientific Research (NWO). Use of synchrotron radiation source was made possible by the agreement between SERC and NWO.

REFERENCES

1. Ort, D. R. and Govindjee (1987) Obschie predstavlenia o preobrazovanie energii pri fotosintezie (General view energy transformation in photosynthesis). In *Fotosintez*, Vol. 1 (Edited by Govindjee), pp. 8–89. Mir, Moskva.
2. Booth, P. J., B. Crystall, I. Ahmad, J. Barber, G. Porter and D. R. Klug (1991) Observation of multiple radical pair states in photosystem 2 reaction centres. *Biochemistry* **30**, 7573–7586.
3. Boxer, S. G. (1990) Mechanisms of long-distance electron transfer in proteins: lessons from photosynthetic reaction centers. *Annu. Rev. Biophys. Biophys. Chem.* **19**, 267–299.
4. van Zandvoort, M. A. M. J., D. Wróbel, A. J. Scholten, D. deJager, G. van Ginkel and Y. K. Levine (1993) Spectroscopic study of chlorophyll *a* in organic solvents and polymerized anhydrous polyvinyl matrix. *Photochem. Photobiol.* **58**(4), 600–606.
5. van Zandvoort, M. A. M. J. (1994) Pigment–polymer matrices as model systems for energy transfer processes between photosynthetic pigments. Thesis, University of Utrecht, the Netherlands.
6. Förster, T. (1948) Zwischenmolekulare Energiewanderungen und Fluorescenz. *Ann. Phys.* **2**, 55–73.
7. Förster, T. (1960) Transfer mechanisms of electronic excitation energy. *Radiat. Res.* Suppl. **2**, 326–339.
8. Knoester, J. and E. van Himbergen (1984) Effect of molecular reorientation on excitation decay due to incoherent energy transfer. *J. Chem. Phys.* **81**, 4380–4388.
9. Dale, R. E., J. Eisinger and W. E. Blumberg (1979) The orientational freedom of molecular probes. The orientation factor in intramolecular energy transfer. *Biophys. J.* **26**, 161–194.
10. Dudkiewicz, J. (1982) Orientation factor and rotation of molecules in luminescent solutions. *J. Luminesc.* **26**, 273–280.
11. Wu, P. and L. Brand (1992) Orientation factor in steady-state and time-resolved resonance energy transfer measurements. *Biochemistry* **31**, 7939–7947.
12. Mersol, J. V., H. Wang, A. Gafni and D. G. Steel (1992) Consideration of dipole orientation angles yields accurate rate equations for energy transfer in the rapid diffusion limit. *Biophys. Soc.* **61**, 1647–1655.
13. Gouterman, M. (1961) Spectra of porphyrins. *J. Mol. Spectrosc.* **6**, 138–163.
14. Weiss, C. (1972) The pi electron structure and absorption spectra of chlorophylls in solution. *J. Mol. Spectrosc.* **44**, 37–80.
15. Edwards, W. D. and M. C. Zerner (1983) Electronic structure of model chlorophyll systems. *Int. J. Quant. Chem.* **13**, 1407–1432.
16. Fragata, M., B. Norden and T. Kurucsev (1988) Linear dichroism (250–700 nm) of chlorophyll *a* and pheophytin *a* oriented in a lamellar phase of glycerylmonooctanoate/H_2O. Character-

ization of electronic transitions. *Photochem. Photobiol.* **47**, 133–143.
17. Norden, B., M. Fragata and T. Kurucsev (1992) X- and Y-polarized spectra of chlorophyll *a* and pheophytin *a* in the red region: resolution enhancement and Gaussian deconvolution. *Aust. J. Chem.* **45**, 1559–1570.
18. Houssier, C. and K. Sauer (1970) Circular dichroïsm and magnetic circular dichroïsm of the chlorophyll and protochlorophyll pigments. *J. Am. Chem. Soc.* **92**, 779–791.
19. Bauman, D. and D. Wróbel (1980) Dichroism and polarized fluorescence of chlorophyll *a*, chlorophyll *c* and bacteriochlorophyll *a* dissolved in liquid crystals. *Biophys. Chem.* **12**, 83–91.
20. Frąckowiak, D., S. Hotchondani and R. M. Leblanc (1983) Effect of electric field on polarized absorption spectra of chlorophyll *a* and chlorophyll *b* in nematic liquid crystals. *Photochem. Photobiol.* **6**, 339–350.
21. Wróbel, D. and M. Kozielski (1988) Resonance Raman spectroscopy of chlorophylls dissolved in liquid crystal matrices. II. Optical properties of chlorophyll *a* in an MBBA + EBBA liquid crystal mixture. *Biophys. Chem.* **29**, 309–315.
22. Langkilde, F. W., E. Thulstrup and J. Michl (1982) The effect of solvent environment on molecular electronic transition moment directions: symmetry lowering in pyrene. *J. Chem. Phys.* **78**(6,II), 3372–3381.
23. Johansson, L. B. Å. (1990) Limiting fluorescence anisotropies of perylene and xanthene derivatives. *S. Chem. Soc. Faraday Trans.* **86**(12), 2103–2107.
24. Shan, Q., X. Dou and B. S. Hudson (1991) Off-axis orientation of the electronic transition moment for a linear conjugated polyene. *Nature* **352**, 703–705.
25. Tolkachev, V. A. and S. P. Pliska (1986) Orientation of the fluorescent transition moment in free molecules of phthalimides and aminoanthraquinones. *Opt. Spectrosc.* **61**(1), 48–51.
26. Ediger, M. D. and M. D. Fayer (1984) Electronic excitation transport in disordered finite volume systems. *J. Phys. Chem.* **88**, 6108–6116.
27. Kaplanova, M. and K. Vacek (1974) Low-temperature fluorescence spectra of chlorophyll *a* solutions. *Photochem. Photobiol.* **20**, 371–375.
28. Kuki, A. and S. G. Boxer (1983) Chlorophyllide substituted hemoglobin tetramers and hybrids: preparation, characterization and energy transfer. *Biochemistry* **22**, 2923–2925.
29. van Gurp, M. and Y. K. Levine (1989) Determination of transition moment directions in molecules of low symmetry using polarized fluorescence. 1. Theory. *J. Chem. Phys.* **8**, 4095–4102.
30. van Gurp, M., G. van Ginkel and Y. K. Levine (1989) Fluorescence anisotropy of chlorophyll *a* and chlorophyll *b* in caster oil. *Biochim. Biophys. Acta* **973**, 405–413.
31. Birks, J. B. (1970) *Photophysics of Aromatic Molecules*. Wiley, New York.
32. van der Heide, U. A., B. Orbons, H. C. Gerritsen and Y. K. Levine (1992) The orientation of transition moments of dye molecules used in fluorescence studies of muscle systems. *Eur. Biophys. J.* **21**, 263–272.
33. Rose, M. E. (1957) *Elementary Theory of Angular Momentum*. Wiley, New York.
34. van Gurp, M., G. van Ginkel and Y. K. Levine (1988) On the distribution of dye molecules in stretched poly(vinyl alcohol). *J. Polym. Sci. B* **26**, 1613–1625.
35. van Gurp, M., H. van Langen, G. van Ginkel and Y. K. Levine (1988) Angle-resolved techniques in studies of organic molecules in ordered systems using polarized light. In *Polarized Spectroscopy of Ordered Systems* (Edited by B. Samori and E. W. Thulstrup), pp. 455–489. Kluwer Academic Publishers, Amsterdam.
36. Nordio, P. L. and U. Segre (1979) Rotational Dynamics. In *The Molecular Physics of Liquid Crystals* (Edited by G. R. Lockhurst and G. W. Gray), pp. 411–425. Academic Press, London.
37. van Gurp, M. and Y. K. Levine (1991) Odd-rank order parameters in nonuniaxial orientational distributions. *Chem. Phys. Lett.* **180**, 349–356.
38. Levine, R. D. and R. B. Bernstein (1975) Thermodynamic approach to collision processes. In *Modern Theoretical Chemistry*, Vol. III, *Dynamics of Molecular Collisions* (Edited by W. H. Miller). Plenum, New York.
39. Fisher, G. (1984) *Vibronic Coupling (Theoretical Chemistry)*. Academic Press, London.
40. Steinberg, I. Z. (1975) In *Biochemical Fluorescence Concepts* (Edited by R. F. Chen and H. Edelhoch), pp. 79–113. Marcel Dekker, New York.
41. Terpstra, W. and W. J. Lambers (1983) Incorporation of chlorophyll *a* and chlorophyllase into artificial membranes. *Photobiochem. Photobiophys.* **6**, 93–100.
42. Inamura, I., H. Ochiai, K. Toki, S. Watanabe, S. Hikino and T. Araki (1983) Preparation and properties of chlorophyll/water-soluble macromolecular complexes in water. Stabilization of chlorophyll aggregates in the water-soluble macromolecule. *Photochem. Photobiol.* **38**, 37–44.
43. Arcioni, A., R. Tarroni and C. Zannoni (1988) Fluorescence depolarization in liquid crystals. In *Polarized Spectroscopy of Ordered Systems* (Edited by B. Samori and E. W. Thulstrup), pp. 421–453. Kluwer Academic Press, Dordrecht.
44. van Gurp, M., T. van Heijnsbergen, G. van Ginkel and Y. K. Levine (1989) Determination of transition moment directions in molecules of low symmetry using polarized fluorescence. 2. Applications to pyranine, perylene and DPH. *J. Chem. Phys.* **90**(8), 4103–4111.
45. Nishijima, Y., Y. Onogi, R. Yamazaki and K. Kawakami (1968) Molecular orientation behaviors in polyvinylalcohol films studied by the fluorescence method. (I) Uniaxial deformations. *Rep. Prog. Polym. Phys. Jpn.* **11**, 407–410.
46. Kooyman, R. P. H. (1980) Complexes and aggregates of chlorophylls. Thesis, Agricultural University of Wageningen, The Netherlands.
47. van Gurp, M. (1988) Molecular orientation of natural dyes in ordered systems studied with polarized light. Thesis, University of Utrecht, The Netherlands.